Integrated analysis identified MARK4 as a prognostic and immunomodulatory biomarker in oral squamous cell carcinoma

XINYUE ZHANG[1-3], XIAOXUE SHEN[1-3], SUJUN HU[1-3] and RUI YAO[1-3]

[1]Department of Pediatric Dentistry, Tianjin Stomatological Hospital, School of Medicine, Nankai University, Tianjin 300041, P.R. China; [2]Tianjin Key Laboratory of Oral and Maxillofacial Function Reconstruction, Tianjin 300041, P.R. China; [3]Department of Pediatric Dentistry, Stomatology Institute of Nankai University, Tianjin 300041, P.R. China

Received April 24, 2026; Accepted July 30, 2026

DOI: 10.3892/ol.2026.15863

Abstract. Oral squamous cell carcinoma (OSCC) is the most common malignancy of the oral cavity and is characterized by high invasiveness and a poor prognosis. Although a number of molecular biomarkers have been investigated, their clinical applications remain limited. Despite microtubule affinity-regulating kinase 4 (MARK4) having been implicated in a number of cancers, its role in OSCC remains unclear. RNA-sequencing data and corresponding clinical information for patients with OSCC were obtained from The Cancer Genome Atlas database. MARK4 expression levels were analyzed in OSCC and corresponding noncancerous tissues. Associations between MARK4 expression and clinicopathological characteristics and survival outcomes, including overall survival (OS), disease-specific survival (DSS) and progression-free interval (PFI), were evaluated using univariate Cox regression and Kaplan-Meier analyses. Immune infiltration was assessed using single-sample Gene Set Enrichment Analysis, Cell-type Identification by Estimating Relative Subsets of RNA Transcripts and Tumor Immune Estimation Resource 2.0 analyses. To evaluate its functional role, two independent small interfering RNA was used to silence MARK4 expression in human squamous carcinoma-3 (HSC-3) cells. Results indicated that MARK4 was notably upregulated in OSCC and was associated with advanced T and clinical stages. High MARK4 expression was associated with poorer OS, DSS and PFI in the unadjusted survival analyses and showed discriminatory ability between tumor and normal tissues (area under the curve=0.841). Functional enrichment analysis indicated that MARK4 and its co-expressed genes were mainly involved in cytoskeletal organization, immune response and metabolic pathways. Immune infiltration analysis showed that MARK4 expression was negatively correlated with $CD8^+$ T, B, dendritic and regulatory T cells. Functional experiments further demonstrated that MARK4 knockdown markedly suppressed HSC-3 cell proliferation and invasion, with minimal effects on cell migration. In conclusion, MARK4 is upregulated in OSCC and is associated with clinicopathological progression, survival outcomes, immune infiltration and tumor-cell aggressiveness. These findings support MARK4 as a potential survival-associated biomarker and candidate therapeutic target; however, its independent prognostic value remains to be established through multivariable analyses and external clinical validation.

Correspondence to: Professor Rui Yao, Department of Pediatric Dentistry, Tianjin Stomatological Hospital, School of Medicine, Nankai University, 75 Dagu Road, Heping, Tianjin 300041, P.R. China
E-mail: yaorui_china@126.com

Key words: microtubule affinity-regulating kinase 4, oral squamous cell carcinoma, prognosis, immune infiltration, biomarker

Introduction

Oral squamous cell carcinoma (OSCC) is an aggressive malignancy of the head and neck region that accounts for >90% of all oral malignancies (1-4). According to Global Cancer Observatory data, 452,205 new cases and 194,108 mortalities from lip and oral cavity cancers were reported worldwide in 2024, with the majority occurring in Asia (5). OSCC typically arises in the mucosal tissues of the oral cavity, tongue and lips. Despite advances in diagnosis and treatment, the 5-year overall survival (OS) rate remains ~50%, largely because of late-stage diagnosis and tumor progression (6,7). Numerous studies have investigated the role of molecular biomarkers in OSCC, including long non-coding RNAs (lncRNAs) and microRNAs (miRNAs) (8-10). Therefore, identifying potential biomarkers associated with OSCC progression may improve prognostic assessment and provide new insights into disease management.

Protein kinases are a large family of enzymes that regulate diverse cellular processes through substrate phosphorylation, including cell proliferation, differentiation, apoptosis, metabolism and signal transduction. The human genome encodes >500 protein kinases that are key for maintaining cellular homeostasis (11). Dysregulation or aberrant activation of these kinases has been implicated in numerous human diseases, particularly cancer, where they contribute to tumor initiation, progression, metastasis and therapeutic resistance (12-19). Consequently, protein kinases have emerged as important biomarkers and therapeutic targets in cancer.

The microtubule affinity-regulating kinase (MARK) family comprises four members, MARK1, MARK2, MARK3 and MARK4, whose genes are located on chromosomes 1, 11, 14 and 19, respectively (20). MARK4 is a serine/threonine protein kinase that phosphorylates microtubule-associated proteins (MAPs) and is broadly expressed in nearly all human tissues (21). It has been implicated in the pathogenesis of numerous diseases, including cancer, Alzheimer's disease, metabolic disorders and cardiovascular conditions (22-25).

MARK4 is aberrantly expressed in a number of human malignancies, including glioma, hepatocellular carcinoma, breast cancer and lung cancer and has been implicated in tumor progression (26). Previous studies have shown that MARK4 contributes to the maintenance of glioblastoma stem cells by regulating neural stem cell proliferation and differentiation (27,28). In addition, MARK4 has been reported to activate oncogenic signaling pathways, such as Wnt/β-catenin signaling and to enhance yes-associated protein/transcriptional coactivator with PDZ-binding motif activity through modulation of the Hippo pathway, thereby promoting tumor cell proliferation and migration (29). These findings have suggested that MARK4 may serve an important role in cancer biology and support its increasing relevance as a potential therapeutic target (30-33). However, the expression patterns and clinical significance of MARK4 in OSCC remain unclear. Therefore, the present study aimed to investigate the expression of MARK4 in OSCC and explore its association with clinicopathological characteristics, prognosis and immune-associated features.

Materials and methods

Data acquisition and processing. RNA-sequencing expression profiles and corresponding clinical annotations for patients with head and neck squamous cell carcinoma (HNSC) were obtained from The Cancer Genome Atlas (TCGA) through the Genomic Data Commons portal (https://portal.gdc.cancer.gov/). Gene expression values were analyzed in transcripts per million (TPM) format and were transformed as $\log_2$(TPM+1) before statistical analysis. Genes with an expression value of zero in all samples were excluded. No additional batch-effect correction was applied after TPM normalization and $\log_2$ transformation.

To focus on OSCC, samples originating from the alveolar ridge, base of tongue, buccal mucosa, floor of mouth, hard palate, oral cavity and oral tongue were selected for OSCC-specific analyses, whereas samples originating from the hypopharynx, larynx, lip, oropharynx and tonsil were excluded. For each clinical analysis, samples lacking the variables required for that specific analysis were excluded using a complete-case approach. Missing clinical values were not imputed, whereas samples with missing information unrelated to a particular analysis were retained.

MARK4 expression analysis. TCGA-HNSC expression dataset used for the unpaired analysis comprised 504 primary tumor samples and 44 TCGA solid-tissue normal samples. Of the 44 normal samples, 33 had corresponding matched primary tumor samples and were included in a separate paired analysis. The remaining 11 normal samples did not have matched tumor samples. For the paired comparison, MARK4 expression was compared between the 33 matched tumor-normal pairs using a two-sided paired Student's t-test. For the unpaired comparison, all 504 primary tumor samples were compared with all 44 TCGA normal tissue samples using a two-sided unpaired Student's t-test. The 33 matched normal samples were included within the group of 44 normal samples in the unpaired analysis and did not constitute an additional independent cohort.

For downstream analyses, patients were stratified into high- and low-MARK4 expression groups according to the median MARK4 expression value within the corresponding analysis cohort. For pan-cancer comparisons, cancer types with <3 samples in either comparison group or with an SD of zero were excluded from statistical testing.

Representative immunohistochemical images of MARK4 protein expression in HNSC and normal oral mucosal tissues were obtained from the Human Protein Atlas (HPA; version 24.0; https://www.proteinatlas.org/) using antibody HPA039186. The normal oral mucosal sample (patient ID: 4008) and the HNSC sample (patient ID: 2547) were obtained from different donors and therefore did not represent matched tissues. These images were used for representative visualization only and no quantitative immunohistochemical scoring was performed.

Survival analysis. Survival analysis of MARK4 mRNA expression across cancer types was performed using univariate Cox proportional hazards regression. Kaplan-Meier curves and log-rank tests were used to evaluate the unadjusted associations between MARK4 expression and survival outcomes in patients with OSCC, including OS, disease-specific survival (DSS) and progression-free interval (PFI). Patients were stratified into high- and low-MARK4 expression groups according to the median expression level. Hazard ratios and corresponding 95% CIs were estimated from the univariate Cox models. Multivariable Cox regression adjusting for age, sex, tumor stage, treatment and other potential clinical confounders was not performed due to incomplete clinical information. Therefore, the survival analyses represent unadjusted associations and were not used to establish MARK4 as an independent prognostic factor. Analyses and visualization were performed using the 'survival' (version 3.3.1; https://cran.r-project.org/package=survival), 'survminer' (version 0.4.9; https://cran.r-project.org/package=survminer) and 'ggplot2' (version 3.4.4; https://cran.r-project.org/package=ggplot2) packages in R (version 4.2.1; https://www.r-project.org/).

Analysis of clinicopathological features. To evaluate the correlation between MARK4 expression and clinicopathological features of OSCC, its association with T-stage, N-stage and clinical stage was further analyzed using data from the TCGA database. Data visualization and statistical analyses were performed using the '*ggplot2*' (version 3.4.4; https://cran.r-project.org/package=ggplot2), '*stats*' (version 4.2.1; https://search.r-project.org/R/refmans/stats/html/stats-package.html) and '*car*' (version 3.1-0; https://cran.r-project.org/package=car) packages in R software.

Functional enrichment analysis. To further elucidate the functional role of MARK4, Gene MANIA (https://genemania.

org/) was employed to identify potential functional partners and construct associated interaction networks. This platform integrates multiple data sources, including physical interactions, co-expression patterns, pathway associations and other functional genomics datasets. The expression correlations between MARK4 and its top ten associated genes were evaluated in OSCC samples using Spearman's correlation analysis. Subsequently, Gene Ontology and Kyoto Encyclopedia of Genes and Genomes pathway enrichment analyses were performed on the selected genes using the 'ggplot2' package (version 3.4.4) in R (version 4.2.1; https://www.r-project.org/).

Correlation analysis of immune cell markers. Based on single-sample Gene Set Enrichment Analysis and Cell-type Identification by Estimating Relative Subsets of RNA Transcripts algorithms implemented in R, the correlation between MARK4 expression and the infiltration of immune cells in patients with OSCC were systematically analyzed. In addition, the Tumor Immune Estimation Resource (TIMER) 2.0 database (http://timer.cistrome.org/) is a public resource that provides comprehensive analysis and visualization of tumor-infiltrating immune cells. In the present study, the TIMER online platform was utilized to assess the correlation between MARK4 expression and the abundance of tumor-infiltrating immune cells in HNSC samples. In addition, the Spearman's correlation test was performed to evaluate the association between MARK4 expression and immune checkpoints.

siRNA transfection. HSC-3 cells were cultured in DMEM (Thermo Fisher Scientific, Inc.) supplemented with 10% FBS (Gibco; Thermo Fisher Scientific, Inc.) and 1% penicillin-streptomycin (Beyotime Biotechnology) at 37˚C in a humidified incubator with 5% CO_2. For siRNA-mediated knockdown, cells were seeded into 6-well plates at a density of $2x10^5$ cells per well and allowed to adhere overnight to reach 50-70% confluence at the time of transfection.

Two siRNAs targeting MARK4, designated siMARK4$^{\#1}$ (sense, 5'-GUUGGUUUAUGUUACUUAAUA-3'; antisense, 5'-CAGUGUAAGUUGAAUUCUAGU-3') and siMARK4$^{\#2}$ (sense, 5'-AUGGAUCAACAUCGGCUAUGA-3'; antisense, 5'-UCAUAGCCGAUGUUGAUCCAU-3'), together with a non-targeting negative-control siRNA (siNC; sense, 5'-UUCUCCGAACGUGUCACGU-3'; antisense, 5'-ACGUGACACGUUCGGAGAA-3'), were separately diluted in Opti-MEM Reduced Serum Medium (Gibco; Thermo Fisher Scientific, Inc.) and prepared for transfection according to the manufacturer's instructions. All siRNAs were synthesized by Beijing Tsingke Biotech Co., Ltd. Lipofectamine® 3000 (Invitrogen; Thermo Fisher Scientific, Inc.) was used as the transfection reagent. Briefly, 7.5 μg siRNA and 3 μl Lipofectamine 3000 were mixed in Opti-MEM, incubated for 15 min at room temperature to allow complex formation and then added dropwise to the cells. The final siRNA concentration was 50 nM. After 6 h of incubation, the medium was replaced with complete DMEM containing 10% FBS. Knockdown efficiency was evaluated 48 h post-transfection through reverse transcription-quantitative PCR (RT-qPCR). Comparisons among the siNC, siMARK4$^{\#1}$ and siMARK4$^{\#2}$ groups were performed using one-way ANOVA followed by Dunnett's multiple-comparisons test, with siNC used as the reference group.

RT-qPCR. Total RNA was isolated from cells using TRIzol reagent (Invitrogen; Thermo Fisher Scientific, Inc.) following the manufacturer's protocol. RNA concentration and purity were assessed spectrophotometrically before reverse transcription. cDNA was synthesized from 1 μg total RNA using a PrimeScript RT Reagent Kit (Takara Biotechnology Co, Ltd.) under the following conditions: 37˚C for 15 min, followed by 85˚C for 5 sec to inactivate the reverse transcriptase. qPCR was subsequently carried out using TB Green Premix Ex Taq II (Takara Biotechnology Co, Ltd.). Amplification was performed with an initial denaturation at 95˚C for 30 sec, followed by 40 cycles consisting of 95˚C for 5 sec and 60˚C for 30 sec. GAPDH served as the endogenous reference gene. Relative expression levels of MARK4 were determined using the comparative $2^{-\Delta\Delta Cq}$ method (34). Each sample was analyzed in three independent replicates. The primer sequences were as follows: MARK4 forward, 5'-AGGTTGCCATCAAGATTATCGAC-3'; reverse, 5'-GATGCGGACTTCTCGGAACAG-3'; GAPDH forward, 5'-GGAGCGAGATCCCTCCAAAAT-3'; reverse, 5'-GGCTGTTGTCATACTTCTCATGG-3'.

Colony formation assay. HSC-3 cells were cultured in DMEM (Gibco; Thermo Fisher Scientific, Inc.) supplemented with 10% FBC (Gibco; Thermo Fisher Scientific, Inc.) and 1% penicillin-streptomycin (Beyotime Biotechnology) at 37˚C in a humidified incubator with 5% CO_2.

For the colony formation assay, exponentially growing HSC-3 cells were trypsinized with 0.25% trypsin-EDTA (Gibco; Thermo Fisher Scientific, Inc.), counted and seeded into 6-well plates at a density of 500 cells per well. After allowing cells to adhere for 24 h, cells were transfected with siMARK4$^{\#1}$, siMARK4$^{\#2}$ and siNC as aforementioned. Cells were subsequently cultured for 10-14 days, with the medium refreshed every 2-3 days, until visible colonies (≥50 cells per colony) were formed.

At the end of incubation, the cells were gently washed twice with PBS, fixed with 4% paraformaldehyde (MilliporeSigma) for 15 min at room temperature and stained with 0.5% crystal violet solution (Beyotime Biotechnology) for 20 min. Excess dye was removed by washing with distilled water and the plates were air-dried at room temperature. Colonies containing ≥50 cells were counted using ImageJ software (version 1.52; National Institutes of Health). The assay was performed in three independent biological experiments. The values obtained from replicate wells were averaged to generate one value for each independent experiment. Image acquisition and colony quantification were performed by an investigator blinded to the treatment allocation.

Transwell invasion assay. Invasive ability of HSC-3 cells was evaluated using 24-well Transwell chambers (8 μm pore size; Corning, Inc.) precoated with Matrigel (Corning, Inc.). Briefly, the upper surface of each insert was coated with Matrigel diluted 1:8 in serum-free DMEM and incubated at 37˚C for 30 min. HSC-3 cells were serum-starved for 12 h, trypsinized and resuspended in serum-free DMEM. A total of $1x10^5$ cells

in 200 μl medium were seeded into the upper chamber, while 600 μl DMEM containing 10% FBS was added to the lower chamber as a chemoattractant. After incubation for 24 h at 37˚C with 5% CO_2, non-invading cells on the upper surface were gently removed with a cotton swab. The invaded cells on the lower surface were fixed with 4% paraformaldehyde for 15 min and stained with 0.5% crystal violet for 20 min at room temperature. The stained cells were washed, air-dried and photographed under an inverted microscope. Invaded cells were counted in five randomly selected non-overlapping fields per insert at 100x magnification using an Olympus IX71 inverted light microscope (Olympus Corporation) and analyzed with ImageJ software (version 1.52). The mean number of invaded cells across the selected fields was calculated for each insert. The experiment was performed independently three times. Measurements from replicate inserts and microscopic fields were averaged to generate one value for each independent biological experiment. Image acquisition and cell counting were performed by an investigator blinded to the treatment allocation.

Wound healing assay. HSC-3 cells were seeded in 6-well plates and grown to near confluence in DMEM supplemented with 10% FBS. Prior to scratching, cells were washed twice with PBS and serum-starved in DMEM containing 1% FBS for 12 h to reduce proliferation-driven closure. A straight wound was made across the cell monolayer using a sterile 200 μl pipette tip; detached cells were removed by gently washing twice with PBS. Fresh serum-free medium was added and the wound area was imaged immediately (0 h) and after 24 h using an inverted light microscope (Olympus Corporation) at the same pre-marked positions. Wound closure was quantified by measuring the wound area at each time point using ImageJ (version 1.52). Wound closure was calculated as follows: Wound closure (%)=[(wound area at 0 h-wound area at 24 h)/wound area at 0 h] x100. Measurements from multiple fields within the same well were averaged before statistical analysis. The assay was performed in three independent biological experiments. Images were acquired at the same pre-marked positions and wound-area quantification was performed by an investigator blinded to the treatment allocation.

Statistical analysis. All statistical analyses and visualizations were performed using R software (version 4.2.1; Posit Software, PBC.) and the aforementioned R packages. Comparisons between pan-cancer or tumor tissues and normal tissues were conducted using the Wilcoxon rank-sum test or the unpaired t-test, as appropriate. Univariate Cox proportional hazards regression was used to evaluate the unadjusted association between MARK4 expression and patient survival. For comparisons of gene expression levels, the Wilcoxon rank-sum test was used for unpaired samples and the Wilcoxon signed-rank test was used for paired samples. No multivariable Cox regression was performed; therefore, the survival results did not establish MARK4 as an independent prognostic factor. The association between MARK4 expression and clinicopathological parameters was assessed using the Kruskal-Wallis test and Dunn's test. Spearman's rank correlation was used to evaluate the association between MARK4 expression and associated genes or immune checkpoint molecules. $P<0.05$ was considered to indicate a statistically significant difference.

Results

MARK4 mRNA expression and its unadjusted associations with survival outcomes across pan-cancer datasets. Pan-cancer analysis revealed that MARK4 expression was notably elevated in numerous tumor types compared with normal tissues (Fig. 1A). Univariate survival analyses were subsequently performed to examine the association between MARK4 expression and survival outcomes. As shown in Fig. 1B-D, elevated MARK4 expression was significantly associated with OS, DSS or PFI in a number of cancer types. High MARK4 expression was associated with shorter OS in adrenocortical carcinoma (ACC), head and neck squamous cell carcinoma, ovarian cancer and uterine corpus endometrial carcinoma (UCEC), whereas it was associated with longer OS in kidney renal clear cell carcinoma (KIRC). Similarly, high MARK4 expression was associated with shorter DSS in ACC, HNSC, mesothelioma and UCEC but with longer DSS in KIRC. High MARK4 expression was also associated with shorter PFI in ACC and HNSC and with longer PFI in glioblastoma multiforme and thymoma. These results represent unadjusted associations and should not be interpreted as evidence that MARK4 is an independent prognostic factor or has tumor-promoting or tumor-suppressive effects in these cancer types.

MARK4 mRNA and protein upregulation in OSCC and HNSC tumors. To further investigate the differential expression of MARK4 in OSCC, both paired and unpaired samples from the TCGA database were analyzed. The results consistently showed that MARK4 expression was significantly higher in OSCC tissues compared with normal tissues (Fig. 1E and F). The present finding was further supported by immunohistochemical staining, which demonstrated higher MARK4 expression in HNSC tissues compared with normal tissues (Fig. 2A). In the unadjusted analyses, high MARK4 expression was found to be significantly associated with poorer OS, DSS and PFI in patients with OSCC (Fig. 2B-D). However, given that potential clinical confounders were not adjusted for, these results indicate an association with survival outcomes but do not establish MARK4 as an independent prognostic factor.

Association between MARK4 expression and clinicopathological characteristics. MARK4 expression was significantly associated with clinical T stage in OSCC. As shown in Fig. 2E, MARK4 levels increased with advancing tumor stage, with significantly higher expression in T3-T4 tumors compared with early-stage tumors. However, no significant differences in MARK4 expression were observed among the different N stages (Fig. 2F). Receiver operating characteristic curve analysis demonstrated that MARK4 exhibited good diagnostic performance in distinguishing OSCC tissues from normal tissues, with an area under the curve=0.841 (95% CI: 0.770-0.911; Fig. 2G). Despite MARK4 having showed moderate discriminatory ability between tumor and normal tissues in the TCGA cohort, the present finding should not be interpreted as evidence of clinical diagnostic utility because external validation and prospective clinical evaluation are lacking. Functional enrichment analysis revealed that MARK4-associated genes were mainly involved in

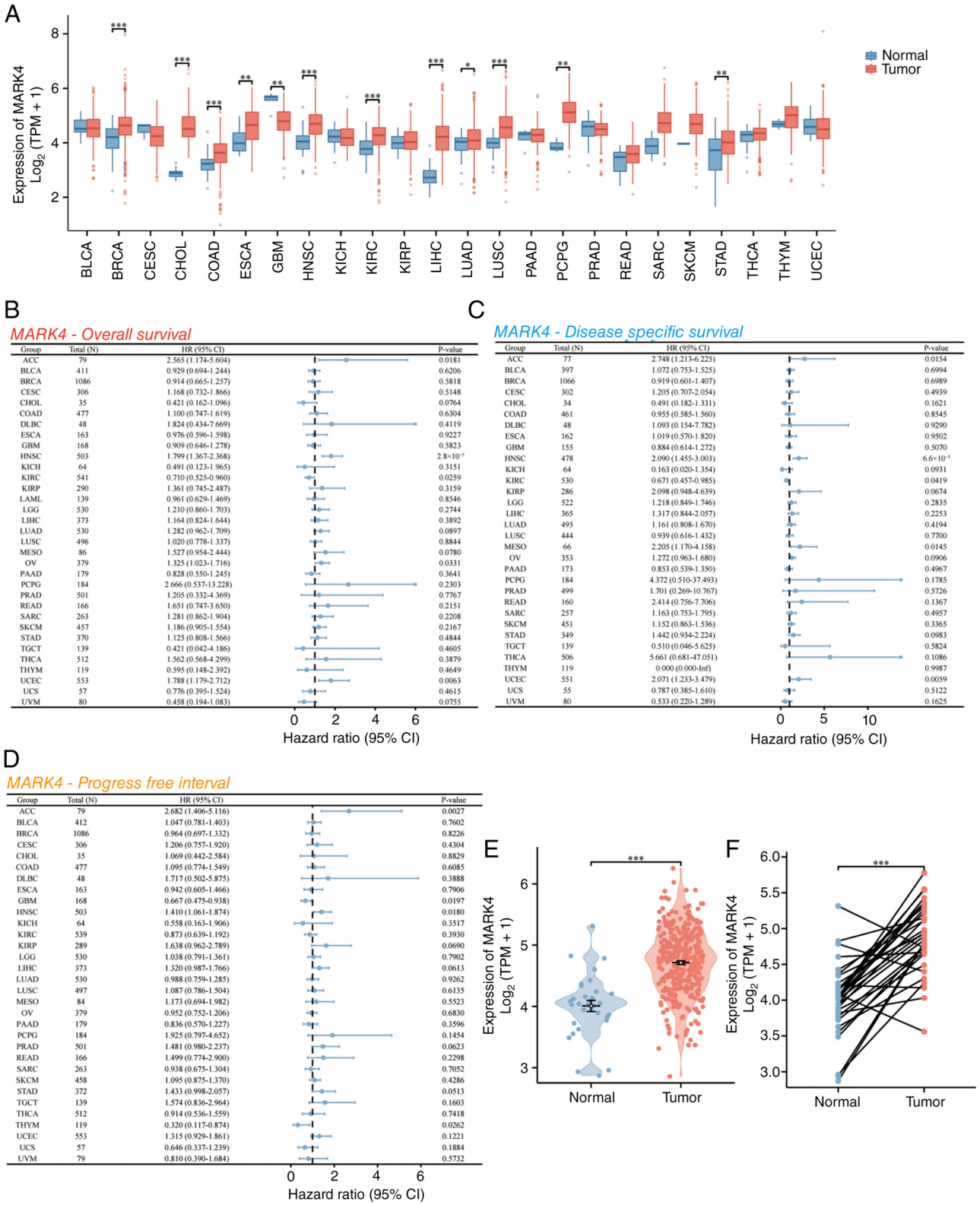

Figure 1. Pan-cancer expression profile of MARK4 and its unadjusted associations with survival outcomes. (A) Expression levels of MARK4 across multiple cancer types (pan-cancer analysis). (B) Association between MARK4 expression and overall survival across pan-cancer cohorts. (C) Association between MARK4 expression and disease-specific survival across pan-cancer cohorts. (D) Association between MARK4 expression and progression-free interval across pan-cancer cohorts. (E) Unpaired and (F) paired comparisons of MARK4 expression between tumor and adjacent normal tissues in OSCC. For comparisons of gene expression levels, the Wilcoxon rank-sum test was used for unpaired samples and the Wilcoxon signed-rank test was used for paired samples. *P<0.05, **P<0.01, ***P<0.001. MARK4, microtubule affinity-regulating kinase 4; TPM, transcripts per million; BLCA, bladder urothelial carcinoma; BRCA, breast invasive carcinoma; CESC, cervical squamous cell carcinoma and endocervical adenocarcinoma; CHOL, cholangiocarcinoma; COAD, colon adenocarcinoma; ESCA, esophageal carcinoma; GBM, glioblastoma multiforme; HNSC, head and neck squamous cell carcinoma; KICH, kidney chromophobe; KIRC, kidney renal clear cell carcinoma; KIRP, kidney renal papillary cell carcinoma; LIHC, liver hepatocellular carcinoma; LUAD, lung adenocarcinoma; LUSC, lung squamous cell carcinoma; PAAD, pancreatic adenocarcinoma; PCPG, pheochromocytoma and paraganglioma; PRAD, prostate adenocarcinoma; READ, rectum adenocarcinoma; SARC, sarcoma; SKCM, skin cutaneous melanoma; STAD, stomach adenocarcinoma; THCA, thyroid carcinoma; THYM, thymoma; UCEC, uterine corpus endometrial carcinoma.

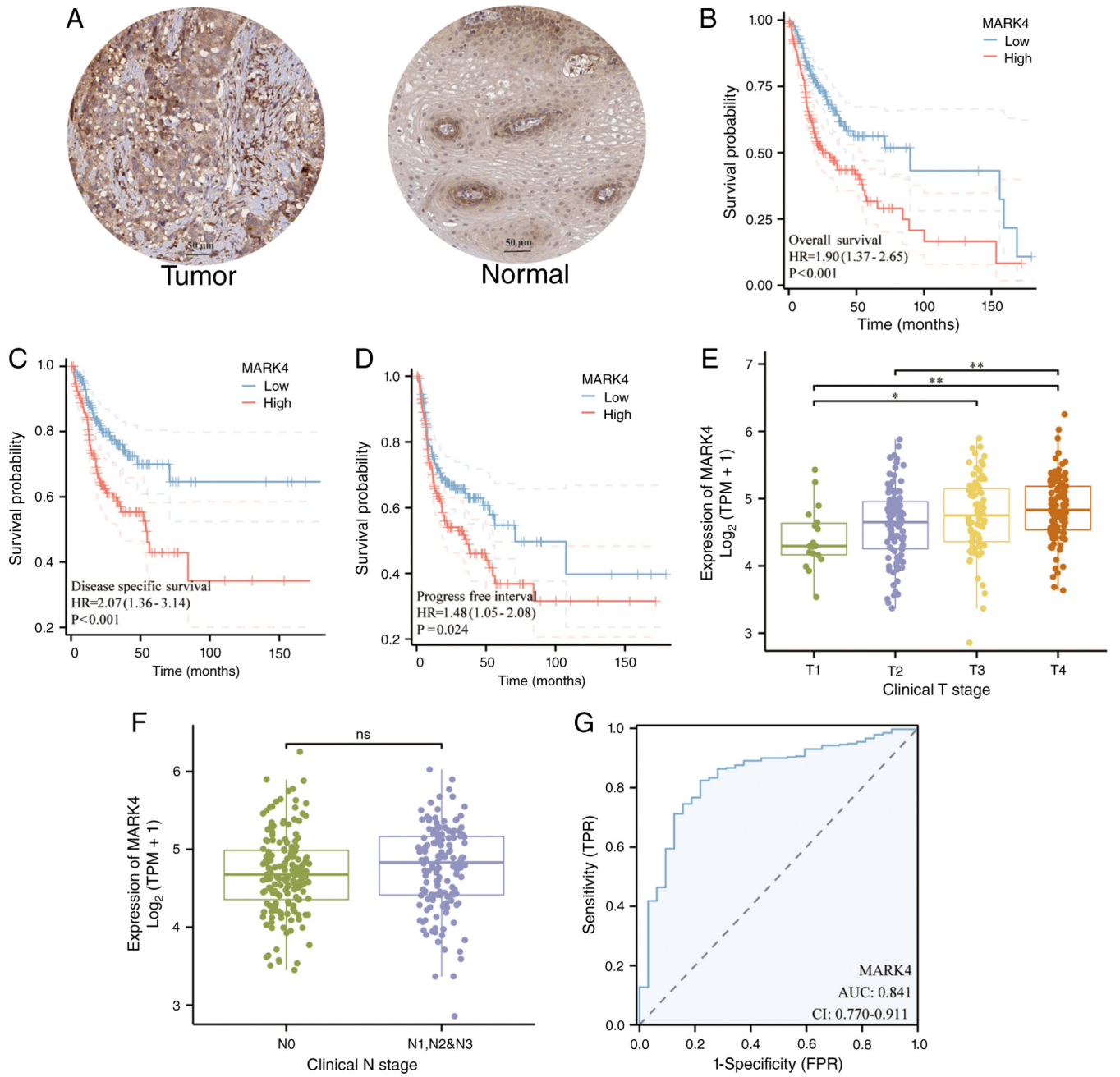

Figure 2. MARK4 is upregulated in OSCC and is associated with survival outcomes and clinicopathological stage. (A) Protein-level expression of MARK4 in OSCC and non-tumor tissues. (B-D) Associations of MARK4 expression with overall survival, disease-specific survival and progression-free interval in OSCC. (E) Association between MARK4 expression levels and tumor T stage. (F) Association between MARK4 expression levels and tumor N stage. (G) Receiver operating characteristic curve illustrating the discriminatory performance of MARK4 expression between TCGA primary tumor tissues and TCGA solid-tissue normal tissues, with an AUC of 0.841. *P<0.05, **P<0.01. ns, not significant; MARK4, microtubule affinity-regulating kinase 4; TPM, transcripts per million; OSCC, oral squamous cell carcinoma; TCGA, The Cancer Genome Atlas; AUC, area under the curve; TPR, true positive rate; FPR, false positive rate.

cytoskeletal organization, 'keratin filament' formation and 'intermediate filament organization' (Fig. 3A; Table SI). The protein-protein interaction network further indicated that MARK4 interacted with numerous proteins associated with cytoskeletal regulation (Fig. 3B and C). Correlation analysis revealed that MARK4 expression was positively associated with a number of cytoskeleton-associated genes, including CAB39, MARK2, NEDD4, PRKCI, USP9X and MARK3. By contrast, no significant correlations were observed with MAPT, PRKAA2, YWHAH and RPIA (Fig. 4).

Association between MARK4 expression and immune cell infiltration. To explore the association between MARK4 and the tumor immune microenvironment in OSCC, immune infiltration analysis was performed. As shown in Fig. 5A, MARK4 expression was notably correlated with a number of immune cell populations. Specifically, MARK4 expression was positively correlated with central memory T cells and natural killer (NK) cells and negatively correlated with a number of immune cell types, including cytotoxic cells, plasmacytoid dendritic cells (pDCs), T cells, B cells, dendritic cells and T helper (Th)

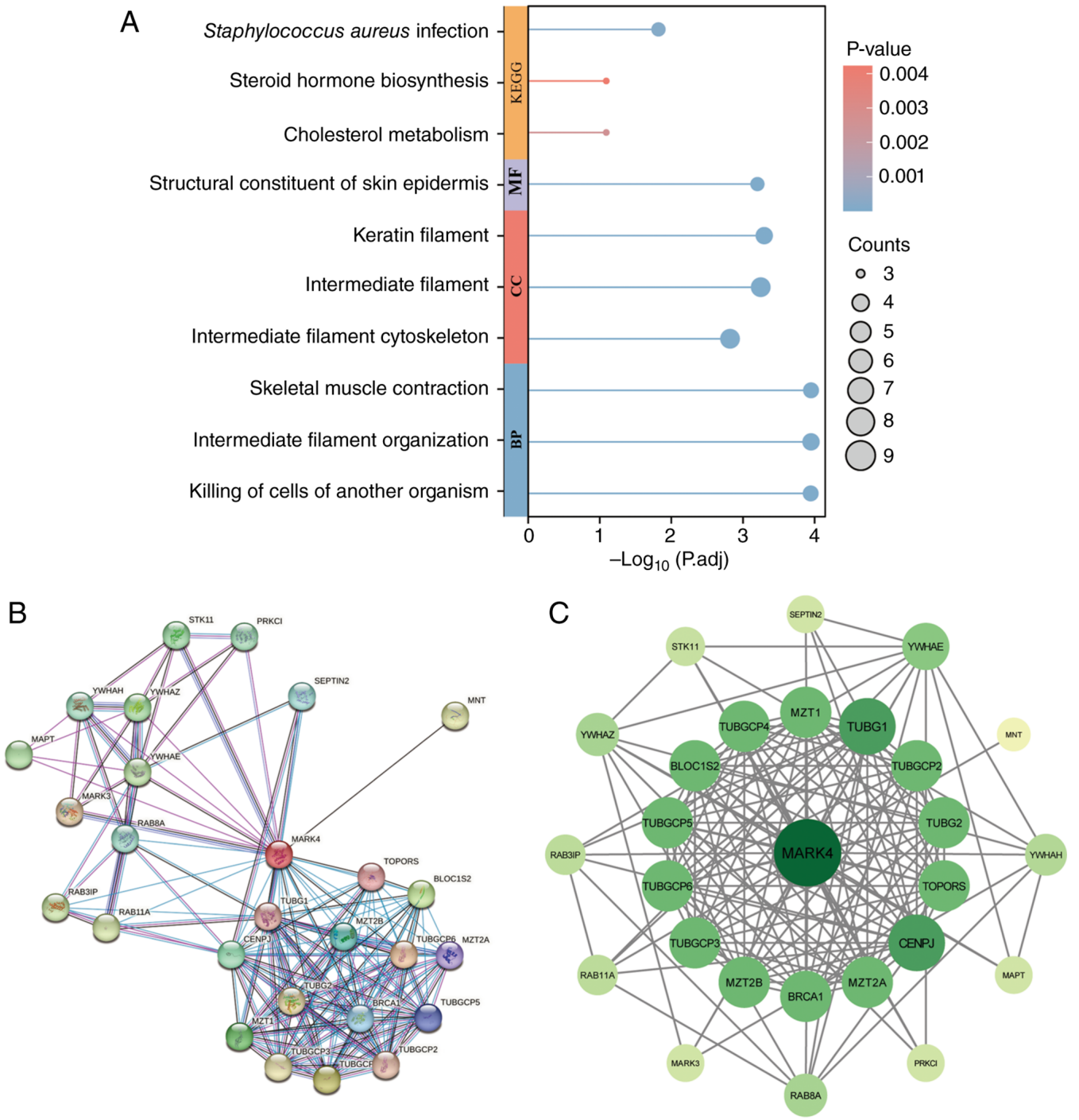

Figure 3. Functional enrichment and correlation network analysis of MARK4-associated genes in OSCC. (A) KEGG pathway enrichment and functional annotation analyses of MARK4-associated genes, highlighting the major pathways and biological processes associated with these genes. (B and C) Predictive analyses of genes co-expressed or functionally associated with MARK4. The size and color intensity of each node are positively correlated with its degree of connectivity in the network, with larger and darker green nodes representing proteins with higher connectivity. KEGG, Kyoto Encyclopedia of Genes and Genomes; MARK4, microtubule affinity-regulating kinase 4; OSCC, oral squamous cell carcinoma; BP, Biological Process; CC, Cellular Component; MF, Molecular Function.

cells. Immune cell composition analysis consistently demonstrated distinct infiltration patterns between the MARK4-high and MARK4-low groups (Fig. 5B). Further comparison of the immune cell enrichment scores revealed that the high-MARK4 group had significantly reduced enrichment of activated DCs, CD8 T cells, cytotoxic cells, DCs, B cells, NK CD56dim cells, pDCs, Th cells, Th17 cells and regulatory T cells compared with the low-MARK4 group (Fig. 5C).

To further investigate the clinical significance of MARK4 in the immune context, survival analyses were performed by stratifying patients according to MARK4 expression and immune cell infiltration levels. As shown in Fig. 6A-G, patients with high MARK4 expression combined with high macrophage M2, mast cell, NK cell or regulatory T cell infiltration tended to exhibit worse OS compared with those exhibiting low MARK4 expression. By contrast, low MARK4

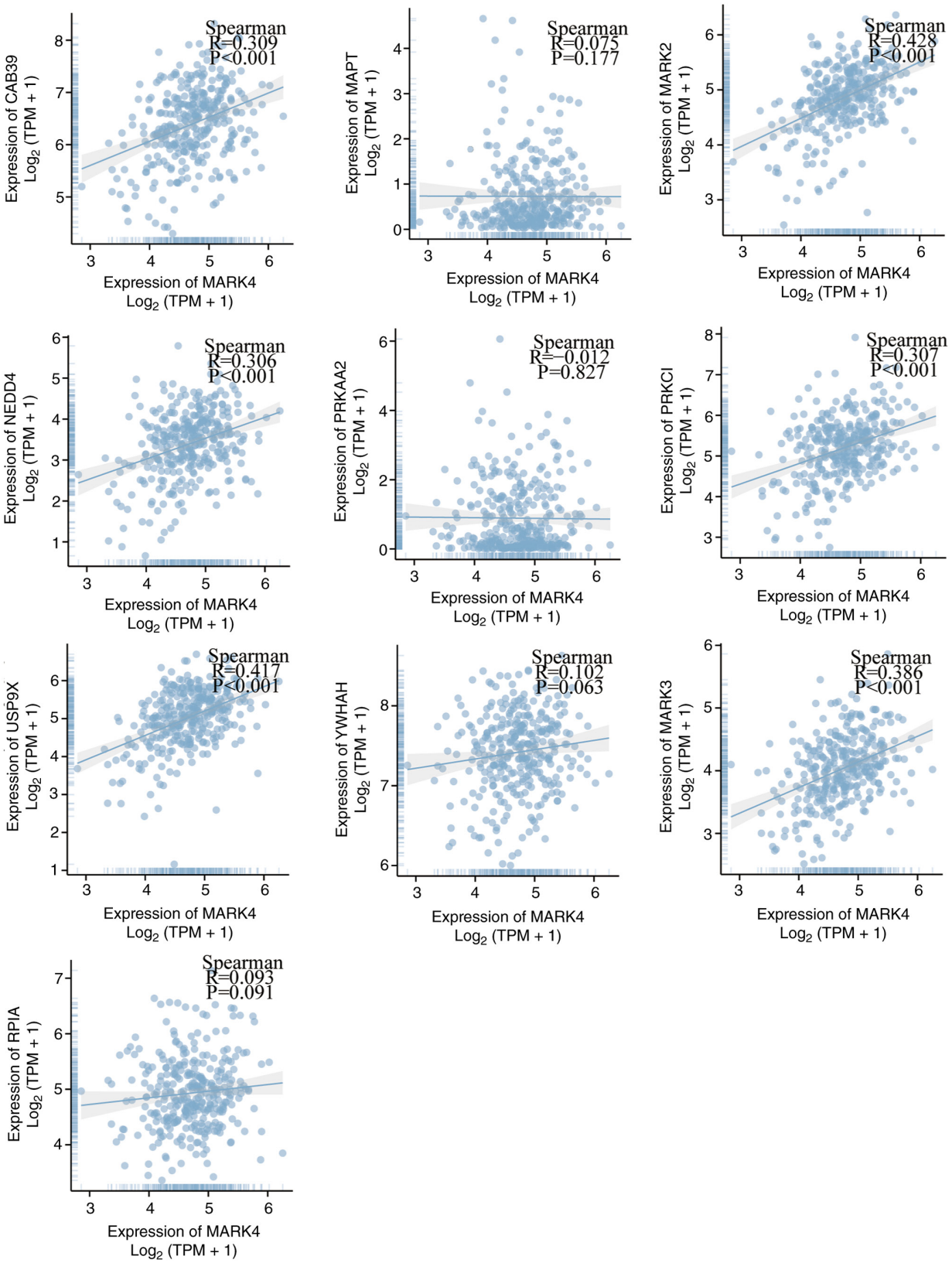

Figure 4. Correlation analysis between MARK4 and key associated genes in oral squamous cell carcinoma. MARK4, microtubule affinity-regulating kinase 4; TPM, transcripts per million.

expression combined with higher estimated infiltration levels of $CD8^+$ T cells or activated $CD4^+$ T cells were associated with more favorable survival outcomes. These stratified survival findings were exploratory and were not adjusted for clinical covariates or potential interactions. They should therefore be interpreted as unadjusted associations rather than evidence that MARK4 modifies the prognostic effects of immune-cell infiltration.

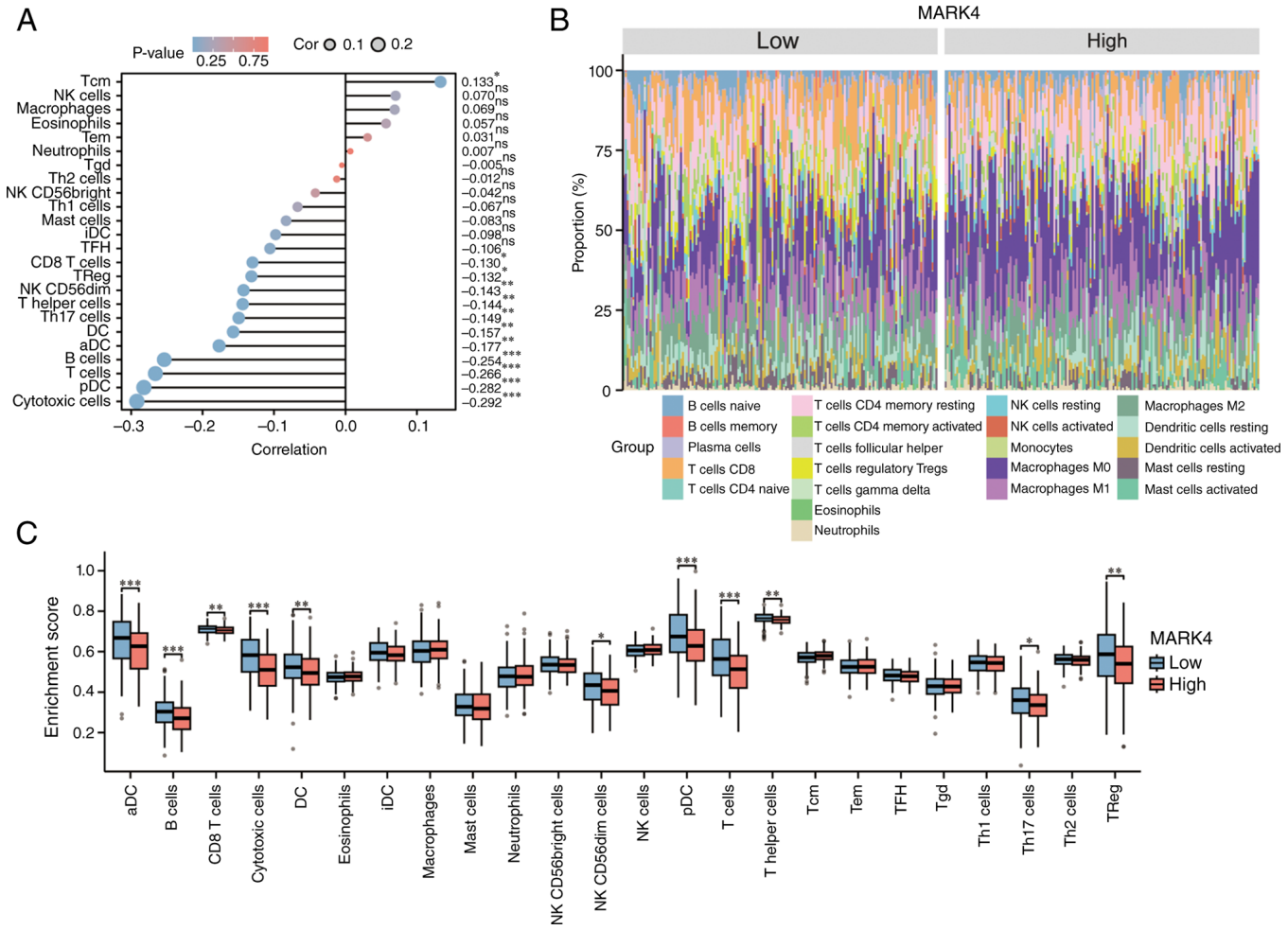

Figure 5. Association between MARK4 expression and immune cell infiltration in OSCC. (A) Correlation between MARK4 expression and the infiltration levels of immune cell populations. (B and C) Immune cell infiltration stratified by different MARK4 expression levels. *P<0.05, **P<0.01, ***P<0.001. ns, not significant; aDC, activated DC; DC, dendritic cell; iDC, immature DC; NK, natural killer; pDC, plasmacytoid dendritic cell; Tcm, central memory T cell; Tem, effector memory T cell; TFH, T follicular helper cell; Tgd, γδ T cell; Th, T helper; TReg, regulatory T cell.

To examine the association between MARK4 expression and immune-associated molecular features, correlations between MARK4 and immune checkpoint-associated genes were analyzed. As shown in Fig. 6H, MARK4 expression was markedly correlated with the expression of multiple immune checkpoint-associated genes, including programmed cell death-1 [programmed death 1 (PD-1)], CD274 (programmed death ligand 1), cytotoxic T-lymphocyte associated protein 4, T-cell immunoreceptor with Ig and ITIM domains, lymphocyte-activation gene 3 and Hepatitis A virus cellular receptor 2. These findings indicate an association between MARK4 expression and immune checkpoint-associated gene expression in OSCC. However, the present correlation analysis does not demonstrate that MARK4 regulates immune checkpoint signaling, promotes immune evasion or affects the response to immune checkpoint blockade.

MARK4 knockdown suppresses HSC-3 cell proliferation and invasion. To explore the functional role of MARK4 in OSCC, HSC-3 cells were transfected with MARK4-specific siRNA. Compared with the NC group, MARK4 mRNA expression was notably reduced in cells transfected with siMARK4, demonstrating the efficient silencing of MARK4 at the transcriptional level (Fig. 7A). Colony formation assays showed that silencing MARK4 significantly reduced both the number and size of colonies compared with the non-targeting control group (Fig. 7B), indicating a notable decrease in proliferative capacity. Similarly, Transwell invasion assays demonstrated a significant reduction in the number of invading cells upon MARK4 silencing (Fig. 7C), suggesting that MARK4 positively regulated the invasive potential of HSC-3 cells. By contrast, wound healing assays revealed no significant difference in the migration rate between MARK4-silenced and control cells over 24 h (Fig. 7D), indicating that MARK4 silencing had a minimal effect on HSC-3 cell motility under these conditions. Collectively, these findings indicate that MARK4 contributes to HSC-3 cell proliferation and invasion; however, its role in cell migration is limited.

Discussion

OSCC is one of the most common and aggressive malignancies of the head and neck, with persistently high incidence and mortality rates worldwide (6). Despite notable progress in diagnostic techniques and therapeutic approaches,

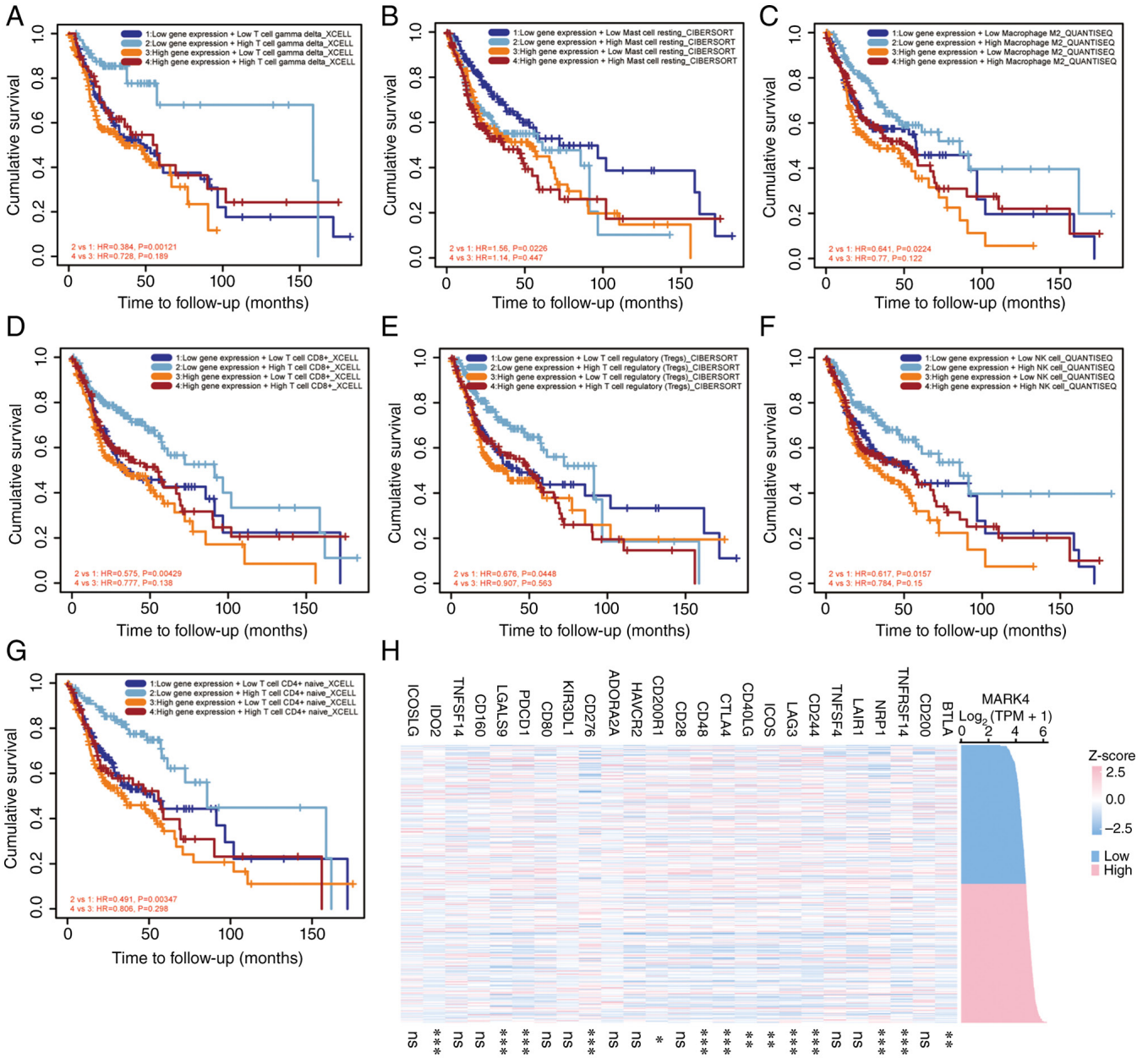

Figure 6. Combined prognostic impact of MARK4 and immune infiltration with immune checkpoint associations in OSCC. (A-G) Combined impact of MARK4 expression and immune cell infiltration on the prognosis of OSCC. (H) Correlations between MARK4 expression and immune checkpoint-associated genes; these associations do not establish regulation of immune checkpoint signaling or immune evasion by MARK4. *P<0.05, **P<0.01, ***P<0.001. ns, not significant; TPM, transcripts per million; MARK4, microtubule affinity-regulating kinase 4; OSCC, oral squamous cell carcinoma; HR, hazard ratio.

the prognosis of patients with OSCC has improved only modestly over the past few decades. Therefore, the identification of specific and sensitive molecular biomarkers is needed to enable early diagnosis and guide more effective treatment strategies. In this context, the present findings suggested that MARK4 may serve as a potential biomarker of OSCC progression and immune characteristics. However, these observations are primarily based on retrospective bioinformatic analyses and limited *in vitro* validation and therefore require further demonstration in independent clinical cohorts and mechanistic studies.

MARK proteins were initially identified based on their ability to phosphorylate MAPs, particularly tau and associated MAPs, thereby regulating microtubule stability and dynamics (35,36). Among the MARK family members, MARK4 has emerged as an important regulator of microtubule organization, cell polarity and cell division and its dysregulation has been implicated in the development and progression of numerous human cancers (37). Previous studies have reported that MARK4 is upregulated in a number of malignancies and is associated with unfavorable clinical outcomes (25,26). For example, MARK4 is markedly upregulated in gastric cancer and has been shown to enhance tumor cell proliferation and migration through activation of the MAPK/ERK signaling pathway (38). Consistent with these findings, the present *in vitro* experiments demonstrated that siRNA-mediated knockdown of MARK4 markedly reduced colony formation and Transwell

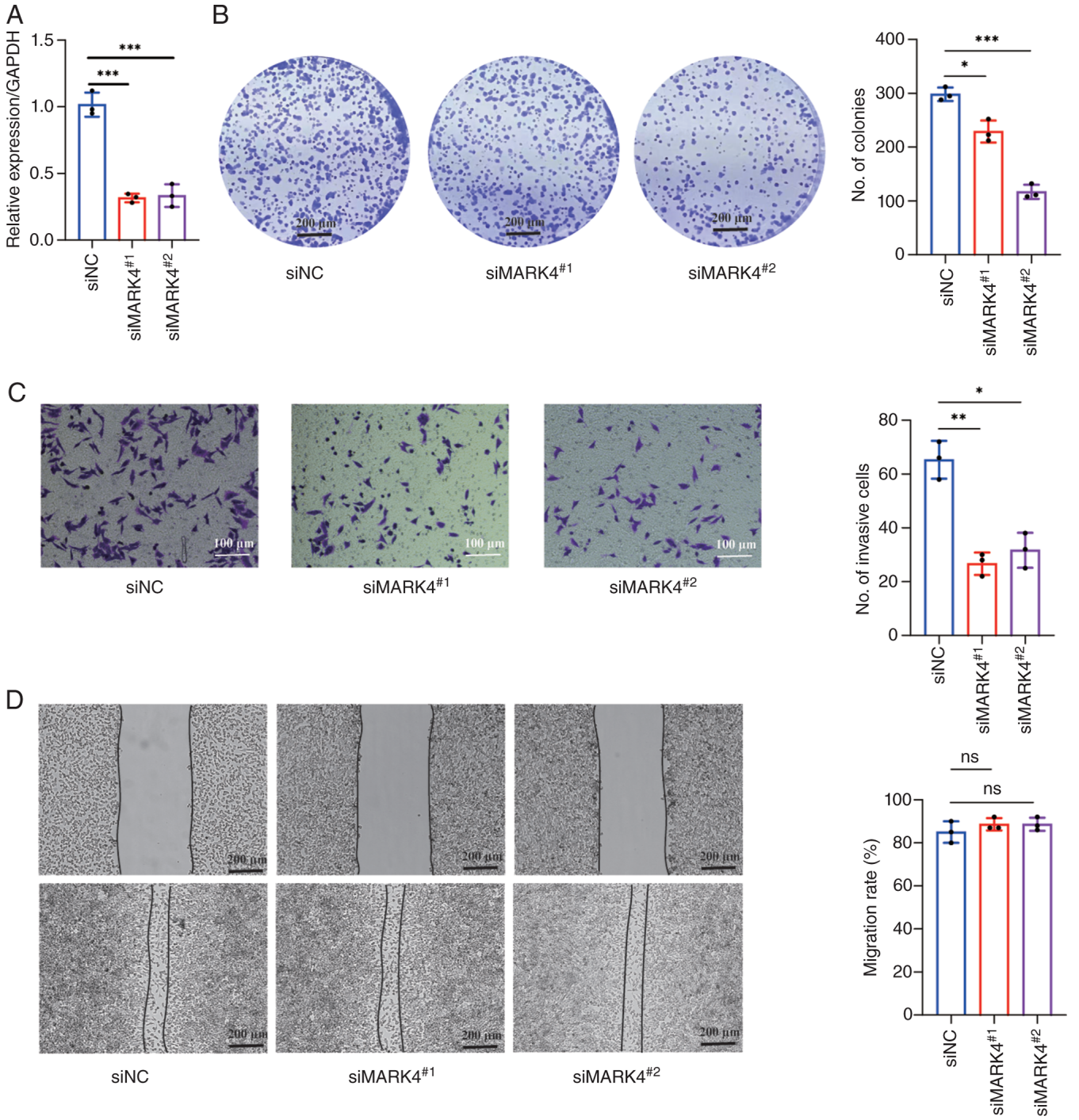

Figure 7. Effects of MARK4 knockdown on the proliferative, invasive and migratory phenotypes of HSC-3 cells. (A) Reverse transcription-quantitative PCR analysis demonstrating the reduction in MARK4 mRNA expression following siMARK4 transfection. (B) Representative images and quantitative analysis of colony formation. (C) Representative images and quantitative analysis of Transwell invasion. (D) Representative images and quantitative analysis of wound closure at 0 and 24 h. Data are presented as the mean ± SD from three independent biological experiments. *P<0.05, **P<0.01, ***P<0.001. ns, not significant; MARK4, microtubule affinity-regulating kinase 4; HSC-3, human squamous carcinoma-3; si, small interfering; NC, negative control.

invasion in HSC-3 cells, suggesting that MARK4 is associated with the proliferative and invasive phenotypes of OSCC cells. By contrast, MARK4 knockdown did not notably affect wound closure in the present wound-healing assay. As wound healing is influenced not only by cell migration but also by cell proliferation and the present experiments were performed in a single cell line without additional mechanistic validation, these results should be interpreted with caution. Further studies using complementary migration assays and mechanistic approaches are required to clarify the role of MARK4 in the regulation of OSCC cell motility.

The present findings further support the notion that MARK4 mRNA is highly expressed in numerous tumor types. In OSCC, MARK4 expression was significantly upregulated in tumor tissues, as consistently observed in

both paired and unpaired samples. In addition, it was found that high MARK4 expression was associated with poorer survival outcomes in the univariate analyses. However, given that these analyses were not adjusted for established clinicopathological prognostic factors, the present findings did not demonstrate that MARK4 provides independent prognostic information. Clinicopathological analysis showed that MARK4 expression levels were positively correlated with the T stage and clinical stage of patients with OSCC, indicating its upregulation with increasing primary tumor progression. However, no significant association was found between MARK4 expression and lymph node metastasis, suggesting that MARK4 primarily promotes primary tumor growth and local infiltration, with limited involvement in lymphatic dissemination.

Functional annotation of MARK4 in the present study indicated that it was primarily localized to keratin filaments, intermediate filaments and the intermediate filament cytoskeleton and played a role in biological processes, including the organization and assembly of intermediate filaments, suggesting a potential role in regulating cell division and cytoskeletal dynamics in cancer cells. Consistent with the present findings, Rovina *et al* (37) reported that MARK4 colocalizes with intermediate filaments, underscoring its role in associating different types of cytoskeletal fibers. In addition, functional experiments in both noncancerous and cancerous cells demonstrated that MARK4 expression in the centrosome and mitotic spindle influenced cell cycle progression. Collectively, these findings support a model in which MARK4 contributes to tumorigenesis by coordinating cytoskeletal organization and regulating the cell cycle.

Tumor progression and the efficacy of immunotherapy are largely influenced by the composition and abundance of immune cells in the tumor microenvironment. The present study found that MARK4 expression was associated with immune cell infiltration in OSCC. Specifically, MARK4 binds to NOD-Like Receptor Pyrin Domain Containing 3 (NLRP3) and facilitates its translocation to the microtubule-organizing center, thereby promoting the assembly of a large inflammasome speck complex (23,39). Furthermore, Wang *et al* (40) proposed that MARK4 inhibition may serve as a potential therapeutic strategy for modulating the progression of NLRP3 inflammasome-associated diseases.

The present study identified associations among MARK4 expression, computationally estimated immune-cell infiltration and survival outcomes in OSCC. In the MARK4-low subgroup, higher estimated infiltration levels of numerous T- and B-cell populations were associated with more favorable survival outcomes, whereas these associations were less evident in the MARK4-high subgroup. These exploratory findings suggest that the association between immune-cell infiltration and survival may differ according to MARK4 expression level. However, the analyses were observational and did not test a statistical interaction in a multivariable model. Therefore, they do not demonstrate that MARK4 remodels the tumor immune microenvironment, suppresses antitumor immunity or modifies the prognostic effects of immune-cell infiltration.

Immune checkpoint blockade, a therapeutic strategy based on the restoration of T cell activity, has demonstrated durable efficacy and notable clinical benefits in a variety of malignancies (41). PD-1 inhibitors have demonstrated notable clinical efficacy in HNSC. The phase Ib KEYNOTE-012 trial showed that pembrolizumab achieved durable antitumor responses with a manageable safety profile in patients with recurrent or metastatic HNSC, leading to the establishment of PD-1 blockade as a key immunotherapeutic strategy for this disease (42). In the present study, MARK4 expression was significantly correlated with the expression of multiple immune checkpoint molecules in OSCC. These present findings suggest that MARK4 is associated with the immune microenvironment in OSCC. However, these correlations were derived from computational analyses and did not establish a causal role for MARK4 in immune regulation or predict responsiveness to immune checkpoint blockade. Therefore, further mechanistic and clinical studies are required to elucidate the biological significance of this association.

The present study exhibits a number of limitations. First, the bioinformatics analyses were based primarily on retrospective public datasets and therefore require validation in independent clinical cohorts. Second, protein expression was evaluated using publicly available HPA immunohistochemistry images, rather than patient-derived specimens. Third, immune cell infiltration was estimated using computational algorithms rather than being experimentally validated by flow cytometry or immunohistochemistry. Fourth, functional experiments were performed in a single OSCC cell line without rescue experiments or *in vivo* validation. Finally, the prognostic analyses were mainly based on univariate associations because incomplete clinical information limited comprehensive multivariable analyses. Therefore, the biological function and clinical significance of MARK4 warrant further investigation.

Acknowledgements

Not applicable.

Funding

No funding was received.

Availability of data and materials

The data generated in the present study may be requested from the corresponding author.

Authors' contributions

XZ, XS and SH performed study conceptualization. RY developed the methodology. XZ and XS performed data validation. SH performed bioinformatics data processing and analysis. XZ and XS conducted the cell biology and molecular biology experiments. RY and SH performed formal data analysis. XZ and XS provided resources and supervision. XZ wrote the manuscript. XZ and XS confirm the authenticity of all the raw data. All authors read and approved the final version of the manuscript.

Ethics approval and consent to participate

Not applicable.

Patient consent for publication

Not applicable.

Competing interests

The authors declare that they have no competing interests.

References

1. Bugshan A and Farooq I: Oral squamous cell carcinoma: Metastasis, potentially associated malignant disorders, etiology and recent advancements in diagnosis. F1000Res 9: 229, 2020.
2. Badwelan M, Muaddi H, Ahmed A, Lee KT and Tran SD: Oral squamous cell carcinoma and concomitant primary tumors, What Do We Know? A review of the literature. Curr Oncol 30: 3721-3734, 2023.
3. Johnson DE, Burtness B, Leemans CR, Lui VWY, Bauman JE and Grandis JR: Head and neck squamous cell carcinoma. Nat Rev Dis Primers 6: 92, 2020.
4. Ladjevac N, Milovanovic M, Jevtovic A, Arsenijevic D, Stojanovic B, Dimitrijevic Stojanovic M, Stojanovic B, Arsenijevic N, Arsenijevic A and Milovanovic J: The role of IL-17 in the pathogenesis of oral squamous cell carcinoma. Int J Mol Sci 24: 9874, 2023.
5. Sung H, Filho AM, Laversanne M, Ferlay J, Siegel RL, Soerjomataram I, Jemal A and Bray F: Global cancer statistics 2024: GLOBOCAN estimates of incidence and mortality worldwide for 34 cancers in 186 countries. CA Cancer J Clin 76: e70090, 2026.
6. Tan Y, Wang Z, Xu M, Li B, Huang Z, Qin S, Nice EC, Tang J and Huang C: Oral squamous cell carcinomas: State of the field and emerging directions. Int J Oral Sci 15: 44, 2023.
7. Meier JK, Schuderer JG, Zeman F, Klingelhöffer Ch, Hullmann M, Spanier G, Reichert TE and Ettl T: Health-related quality of life: A retrospective study on local vs. microvascular reconstruction in patients with oral cancer. BMC Oral Health 19: 62, 2019.
8. Blatt S, Krüger M, Ziebart T, Sagheb K, Schiegnitz E, Goetze E, Al-Nawas B and Pabst AM: Biomarkers in diagnosis and therapy of oral squamous cell carcinoma: A review of the literature. J Craniomaxillofac Surg 45: 722-730, 2017.
9. Sur S, Davray D, Basu S, Kheur S, Pal JK, Nagar S, Sanap A, Rudagi BM and Gupta S: Novel insights on oral squamous cell carcinoma management using long non-coding RNAs. Oncol Res 32: 1589-1612, 2024.
10. Piao Y, Jung SN, Lim MA, Oh C, Jin YL, Kim HJ, Nguyen QK, Chang JW, Won HR and Koo BS: A circulating microRNA panel as a novel dynamic monitor for oral squamous cell carcinoma. Sci Rep 13: 2000, 2023.
11. Fabbro D, Cowan-Jacob SW and Moebitz H: Ten things you should know about protein kinases: IUPHAR Review 14. British J Pharmacology 172: 2675-2700, 2015.
12. Fassl A, Geng Y and Sicinski P: CDK4 and CDK6 kinases: From basic science to cancer therapy. Science 375: eabc1495, 2022.
13. Fleming Martinez AK and Storz P: Protein kinase D1-A targetable mediator of pancreatic cancer development. Biochim Biophys Acta Mol Cell Res 1871: 119646, 2024.
14. García-Aranda M and Redondo M: Protein kinase targets in breast cancer. Int J Mol Sci 18: 2543, 2017.
15. Bucko PJ and Scott JD: Drugs that regulate local cell signaling: AKAP targeting as a therapeutic option. Annu Rev Pharmacol Toxicol 61: 361-379, 2021.
16. Rosenthal KJ, Gordan JD and Scott JD: Protein kinase A and local signaling in cancer. Biochem J 481: 1659-1677, 2024.
17. Smiles WJ, Catalano L, Stefan VE, Weber DD and Kofler B: Metabolic protein kinase signalling in neuroblastoma. Mol Metab 75: 101771, 2023.
18. Glebov-McCloud AGP, Saide WS, Gaine ME and Strack S: Protein Kinase A in neurological disorders. J Neurodevelop Disord 16: 9, 2024.
19. Tabit CE, Shenouda SM, Holbrook M, Fetterman JL, Kiani S, Frame AA, Kluge MA, Held A, Dohadwala MM, Gokce N, *et al*: Protein Kinase C-β contributes to impaired endothelial insulin signaling in humans with diabetes mellitus. Circulation 127: 86-95, 2013.
20. Anwar S, Shahwan M, Hasan GM, Islam A and Hassan MI: Microtubule-affinity regulating kinase 4: A potential drug target for cancer therapy. Cell Signal 99: 110434, 2022.
21. Alam M, Ahmed S, Abid M, Hasan GM, Islam A and Hassan MI: Therapeutic targeting of microtubule affinity-regulating kinase 4 in cancer and neurodegenerative diseases. J Cell Biochem 124: 1223-1240, 2023.
22. Yu X, Chen X, Amrute-Nayak M, Allgeyer E, Zhao A, Chenoweth H, Clement M, Harrison J, Doreth C, Sirinakis G, *et al*: MARK4 controls ischaemic heart failure through microtubule detyrosination. Nature 594: 560-565, 2021.
23. Li X, Thome S, Ma X, Amrute-Nayak M, Finigan A, Kitt L, Masters L, James JR, Shi Y, Meng G, *et al*: MARK4 regulates NLRP3 positioning and inflammasome activation through a microtubule-dependent mechanism. Nat Commun 8: 15986, 2017.
24. Mumtaz, Ahmed F, Rabbani SA, El-Tanani M, Najmi AK, Ali J and Khan MA: Tauopathy in AD: Therapeutic potential of MARK-4. Curr Alzheimer Res 21: 779-790, 2024.
25. Heidary Arash E, Shiban A, Song S and Attisano L: MARK4 inhibits Hippo signaling to promote proliferation and migration of breast cancer cells. EMBO Rep 18: 420-436, 2017.
26. Pardo OE, Castellano L, Munro CE, Hu Y, Mauri F, Krell J, Lara R, Pinho FG, Choudhury T, Frampton AE, *et al*: miR-515-5p controls cancer cell migration throughMARK4 regulation. EMBO Rep 17: 570-584, 2016.
27. Magnani I, Novielli C, Fontana L, Tabano S, Rovina D, Moroni RF, Bauer D, Mazzoleni S, Colombo EA, Tedeschi G, *et al*: Differential signature of the centrosomal MARK4 isoforms in glioma. Anal Cell Pathol (Amst) 34: 319-338, 2011.
28. Naqvi AAT, Jairajpuri DS, Hussain A, Hasan GM, Alajmi MF and Hassan MI: Impact of glioblastoma multiforme associated mutations on the structure and function of MAP/microtubule affinity regulating kinase 4. J Biomol Struct Dyn 39: 1781-1794, 2021.
29. Jenardhanan P, Mannu J and Mathur PP: The structural analysis of MARK4 and the exploration of specific inhibitors for the MARK family: A computational approach to obstruct the role of MARK4 in prostate cancer progression. Mol BioSyst 10: 1845-1868, 2014.
30. Anwar S, Khan S, Shamsi A, Anjum F, Shafie A, Islam A, Ahmad F and Hassan MI: Structure-based investigation of MARK4 inhibitory potential of Naringenin for therapeutic management of cancer and neurodegenerative diseases. J Cell Biochem 122: 1445-1459, 2021.
31. Peerzada MN, Khan P, Khan NS, Avecilla F, Siddiqui SM, Hassan MI and Azam A: Design and development of Small-molecule Arylaldoxime/5-Nitroimidazole hybrids as potent inhibitors of MARK4: A promising approach for Target-based cancer therapy. ACS Omega 5: 22759-22771, 2020.
32. Ahmed S, Queen A, Irfan I, Siddiqui MN, Abdulhameed Almuqdadi HT, Setia N, Ansari J, Hussain A, Hassan MI and Abid M: Vanillin-Isatin Hybrid-induced MARK4 inhibition as a promising therapeutic strategy against hepatocellular carcinoma. ACS Omega 9: 25945-25959, 2024.
33. Li F, Liu Z, Sun H, Li C, Wang W, Ye L, Yan C, Tian J and Wang H: PCC0208017, a novel small-molecule inhibitor of MARK3/MARK4, suppresses glioma progression in vitro and in vivo. Acta Pharm Sin B 10: 289-300, 2020.
34. Livak KJ and Schmittgen TD: Analysis of relative gene expression data using real-time quantitative PCR and the 2(-Delta Delta C(T)) method. Methods 25: 402-408, 2001.
35. Matenia D and Mandelkow EM: The tau of MARK: A polarized view of the cytoskeleton. Trends Biochem Sci 34: 332-342, 2009.
36. Peng N and Nakamura F: Microtubule-associated proteins and enzymes modifying tubulin. Cytoskeleton (Hoboken) 80: 60-76, 2023.
37. Rovina D, Fontana L, Monti L, Novielli C, Panini N, Sirchia SM, Erba E, Magnani I and Larizza L: Microtubule-associated protein/microtubule affinity-regulating kinase 4 (MARK4) plays a role in cell cycle progression and cytoskeletal dynamics. Eur J Cell Biol 93: 355-365, 2014.

38. Ma F, Yao J, Niu X, Zhang J, Shi D and Da M: MARK4 promotes the malignant phenotype of gastric cancer through the MAPK/ERK signaling pathway. Pathol Res Pract 261: 155471, 2024.
39. Gao W, Zeng ZJ, Lin X, Wang PQ, Chen X and Li Y: Discovery of a novel Mark4 antagonist from safflower to improve ischemic stroke by inhibiting microglial Nlrp3 inflammasome activation. Phytomedicine 144: 156909, 2025.
40. Wang L, Pu W, Wang C, Lei L and Li H: Microtubule affinity regulating kinase 4 promoted activation of the NLRP3 inflammasome-mediated pyroptosis in periodontitis. J Oral Microbiol 14: 2015130, 2021.
41. Ferris RL, Blumenschein GJ, Fayette J, Guigay J, Colevas AD, Licitra L, Harrington K, Kasper S, Vokes EE, Even C, *et al*: Nivolumab for recurrent squamous-cell carcinoma of the head and neck. N Engl J Med 375: 1856-1867, 2016.
42. Seiwert TY, Burtness B, Mehra R, Weiss J, Berger R, Eder JP, Heath K, McClanahan T, Lunceford J, Gause C, *et al*: Safety and clinical activity of pembrolizumab for treatment of recurrent or metastatic squamous cell carcinoma of the head and neck (KEYNOTE-012): An open-label, multicentre, phase 1b trial. Lancet Oncol 17: 956-965, 2016.